MODELING INTERACTIONS BETWEEN FIRE AND ATMOSPHERE IN DISCRETE ELEMENT FUEL BEDS

J2.2

Rodman Linn[1*], Judith Winterkamp[1], Carleton Edminster[2], Jonah Colman[1], Michael Steinzig[1]

[1] Earth and Environmental Sciences Division
Los Alamos National Laboratory, Los Alamos, NM 87545
[2] USDA Forest Service, Rocky Mountain Research Station

1. INTRODUCTION

Wildfires are comprised of a complex set of physical and chemical processes, some of whose interactions depend on the coupling between atmospheric flows, the fire, and the vegetation structure. This coupling affects many aspects of the wildfire, such as the balances between different modes of heat transfer, the turbulent mixing which brings gaseous reactants together, and the shape of the fire perimeter.

The ongoing development of the HIGRAD/FIRETEC wildfire modeling system presents a new tool for the investigation of coupled atmosphere/fire/fuel interactions. This modeling framework is composed of an atmospheric model, HIGRAD (Reisner et. al.: 1999, Reisner et. Al. 2000), which is designed to capture high gradients in quantities such as temperature and velocity, and a wildfire model, FIRETEC (Linn, 1997). FIRETEC is based on conservation of mass, momentum, species, and energy. HIGRAD/FIRETEC has been used to examine fire behavior and the interaction between the fire and atmosphere in a number of idealized simulations, including idealized grass fires and homogenized understory and canopy simulations. These idealized simulations show strong interaction between fire, atmosphere and vegetation structure.

We have begun using HIGRAD/FIRETEC to simulate fires in more realistic representations of vegetation, starting with fires in fuelbeds that resemble ponderosa pine forests. The structure of the vegetation in these simulations is based on individual tree data measured at experimental sites near Flagstaff, Arizona. These types of simulations give us a chance to examine the interaction of wind and fire in discontinuous fuel beds and, more specifically, to investigate the role that the canopy structure might serve in such fires.

In this text we introduce some of the conceptual models that we have used to translate the measured tree data into discrete fuel elements that can be used in FIRETEC. We describe a few simulations that have been performed with these discrete fuel elements (we shall refer to the fuel elements as trees even though they are in fact very crude representations of trees). We will illustrate some of the results that can come from these types of simulations in hopes that they will provide the seeds for future research directions. We will not go into details concerning the formulation of FIRETEC or HIGRAD or their numerical implementation since most of these details can be found in (Linn: 1997, Linn et. al.: 2002, Reisner et. al.: 1999).

2. FUEL REPRESENTATION

HIGRAD/FIRETEC is a finite volume computer program that uses a structured three-dimensional grid to describe evolving, spatially varying quantities such as temperature, velocity of the gaseous species as well as characteristics of the fuel. Fuel is described by assigning mean or bulk quantities such as fine fuel surface area per unit volume, moisture ratio, and density to each cell in the three-dimensional grid. This methodology allows HIGRAD/FIRETEC to simulate complex fuel beds that are vertically and horizontally nonhomogeneous.

Researchers from the USDA Forest Service (led by Carleton Edminster) and Northern Arizona University (led by John Bailey) measured canopy vegetation characteristics on a number of 20 m by 50 m

* Corresponding author address:
Rodman Linn
Los Alamos National Laboratory,
MS D401, Los Alamos, New Mexico 87545
E-mail: rrl@lanl.gov

plots near Flagstaff, Arizona. Data was collected for each tree within the plots as a part of the Fire/Fire Surrogate program, which is funded by the Joint Fire Sciences Program with additional funding from Rocky Mountain Research Station. The data that was collected included tree height, height to live crown, height to dead crown, diameter of the crowns in two directions, and diameter of the trunks at breast height for each tree within the plots. After this extensive sampling effort, the challenge was to convert the collected data into three-dimensional fuel distributions that could be used in HIGRAD/FIRETEC to simulate a fire burning through trees similar to those measured. For this initial effort, we chose to work with a simple bulk averaged structural model for a ponderosa pine tree. In the future, we hope to explore other structural models in collaboration with researchers such as Joe Scott.

We developed a conceptual model for a ponderosa pine tree based on the notions that the majority of the fine fuels form a shell around the outside of the canopy that can be described with paraboloids. We assumed that the density of the fine fuels declines from the outside of the tree to the center of the tree (especially near the bottom of the canopy.) We also chose to treat the trees as if they were axisymmetric.

With these ideas in mind, we used a series of parabolic profiles to generate a function that describes the distribution of the mass of an idealized tree. From these profiles and the locations of the trees, we can establish the bulk density of fine vegetation in each cell of the three-dimensional HIGRAD/FIRETEC mesh. Each cell in the mesh can contain parts of one or more trees or be in a location where there are no trees. The first step in resolving each tree is to define the locations that are inside the tree perimeter. The formulation that we used to define the interior of the tree crown is shown in equation 1 in terms of a height above the ground, z, and a distance from the center of the particular tree, r.

$$\frac{h}{R^2}\left[r^2\right]+C \le crown_{\text{interior}} \le \frac{d}{R^2}\left[r^2\right]+H \quad (1)$$

The variables are illustrated in Fig. 1. h and d are used to scale the parabolic shapes that form the top and bottom of the crown, and when summed they equal the difference between the height of the tree, H, and the height to crown, C. We are currently using a value of $h = d/4$. R is the crown radius at its widest point. The density in the interior of the tree, ρ_{canopy}, is approximated by the equation

$$\rho_{canopy} = \left[1 - \frac{z - \left(C + \frac{d}{R^2} r^2\right)}{H - C}\right] \rho_{\max}. \quad (2)$$

By requiring the integral of this function over the interior of the crown to be equal to the volume of the crown multiplied by an average crown bulk density (bulk density of the crown of a single tree), we get the expression in equation 3.

$$\rho_{\max} = \frac{6}{5}\rho_{avg} \quad (3)$$

The average crown density for individual trees was chosen to be .4 Kg/m^3. These expressions provide a method for converting standard tree canopy measurements for

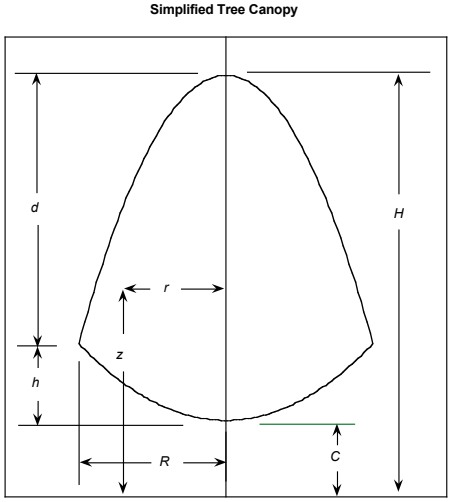

Figure 1. This diagram shows a two-dimensional cross section of the axisymmetrical three-dimensional shape that we use to describe the crowns of trees in our simulations. A location inside the crown is specified by z and r. C, R, and, H are specified from the field data.

ponderosa pine trees into a spatial distribution of vegetation bulk density.

With the expressions given above, there are a number of ways that we could estimate the average value for a computational cell. We chose to numerically integrate the bulk density function over the portion of the cell that is within the interior of the canopy, and divide by the volume of the cell in order to get an average bulk density for the cell.

Since the sampled plots were only 20 m by 50 m in size and we wished to simulate fires over much larger regions, we chose to distribute the trees randomly in a number of adjacent 20 m by 50 m domains. This methodology allows us to generate large stands of trees without having the periodic arrangement that would occur if we used the same locations for the trees within each 20 m by 50 m plot.

There are many ways to approximate the distribution of ground fuels under the canopies. We chose a simplified algorithm for this text but anticipate the inclusion of more sophisticated algorithms in the future. The current model for ground fuel includes a load for grass and a load for litter. We make the assumption that the grass fuel falls off with the amount of canopy above it, s, while the litter load increases with the amount of canopy above it. This model is described by the following equation 4,

$$\rho_{ground} = \rho_{grass} e^{-c_g s} + \rho_{litter}\left(1 - e^{-c_l s}\right), \qquad (4)$$

where ρ_{ground} is the density of the combined grass and litter, ρ_{grass} is the bulk density of the grass in the lowest cell when there is no canopy above it, ρ_{litter} is a assumed maximum litter bulk density in the ground cell under maximum canopy cover, and c_g and c_l are nondimensional proportionality constants. The values of ρ_{grass}, ρ_{litter}, c_g, and c_l were chosen to be .464 kg/m^3, 22 kg/m^3, 5, and 5 respectively for the set of simulations described in this text. It should be noted that the bulk density of the grass and litter is a function of the vertical resolution of the lowest cell since it is the mass of the fuel divided by the volume of the cell and the height of the grass or litter bed is often less than the height of the cell.

3. SIMULATIONS

For the purpose of demonstrating the coupled fire/atmosphere interactions in a fuel bed made of trees similar to those near Flagstaff, we performed four simulations with different canopy and understory configurations. In each of the simulations we ignited a fire near a 60 m wide fuel break (area with no fuel). The fire was blown with a 6 m/s wind across a 20 m grass area toward a forested region. The forested region is 220 m wide, with a 20 m area of grass on the far side of the forest. The total horizontal domain of the simulations is 320 m by 320 m, including the forest, the grassland, and the fuel break. The horizontal resolution near the ground is 2 m, and the vertical resolution is approximately 1.5 m at the ground.

In the first simulation, which we will refer to as the "Full" forest simulation, the canopy is created using the methodology described above over a 220 m by 320 m region. This simulation is depicted in Fig. 2. The canopy in this simulation consists of over 5000 trees. The canopy bulk density over the forested region is approximately 0.24 Kg/m^3.

The forest in the second simulation was derived from the canopy in the first simulation by removing every tree that had a trunk diameter of less than 28 m at breast height. This trunk diameter is one piece of the field data that was collected for each tree. The diameter threshold was chosen arbitrarily for testing purposes. An image from this simulation is shown in Fig. 3. There are only about 1000 trees in this forested area. The canopy bulk density over the forested region is approximately .055 Kg/m^3. We will refer to this simulation as the "Thin" simulation for the rest of the text.

The third simulation, hereafter called the "Patches" simulation, contains a canopy derived from that used in the full forest case. In this simulation, trees were removed to leave patches of varying sized trees. The patches were placed arbitrarily, with the mean spacing between patches on the order of 50 m and the average radius of the patches approximately 15 m. An image from this simulation is shown in Fig. 4. The canopy bulk density over the forested region is approximately .066 Kg/m^3.

The canopy used in the fourth simulation is the same as the canopy in the patches

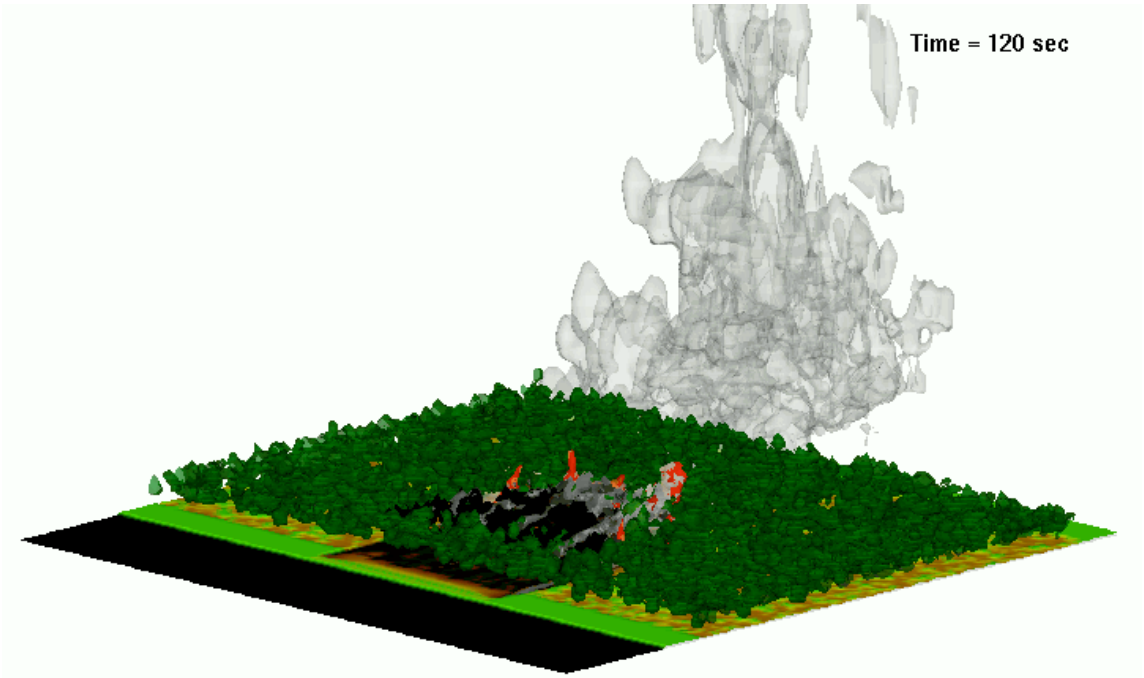

Figure 2. Image from the Full simulation 120 seconds after ignition. The colors on the horizontal plane indicate bulk ground fuel density, with black being no fuel and bright green being 1 kg/m3 (.7 m tall grass). The brown areas are locations where there is less grass, but some fuel litter. The dark green isosurfaces show the tree locations, and the black isosurfaces show parts of the canopy that has been significantly burned. The orange, red, and grey isosurfaces indicate regions of hot gases.

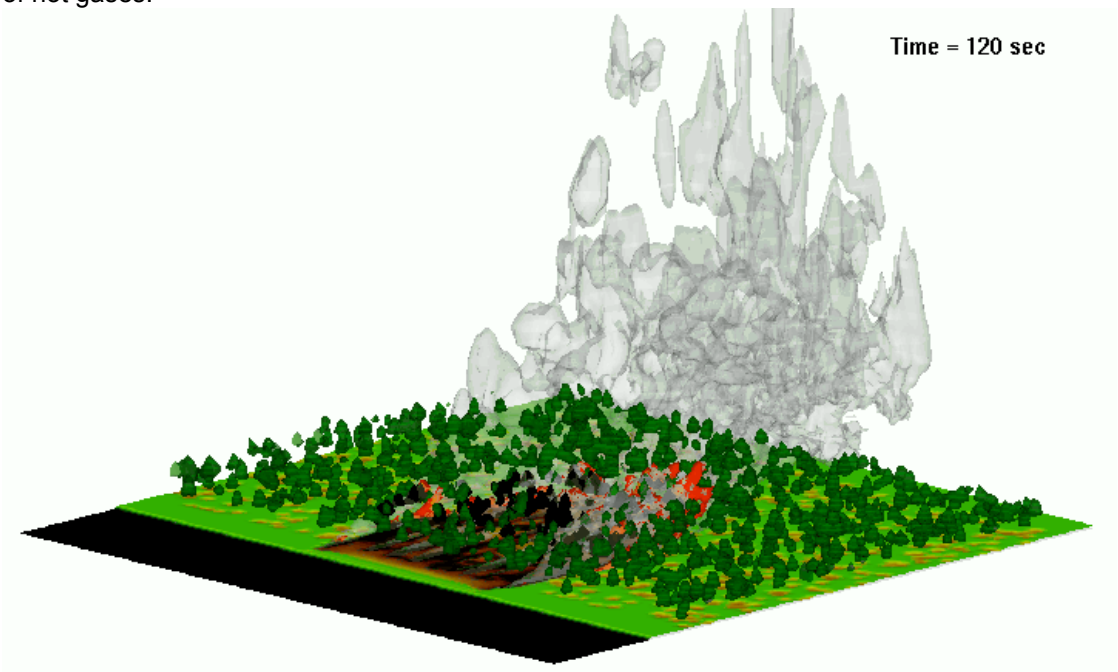

Figure 3. Image from the Thin simulation 120 seconds after ignition. The colors in this image are similar to those in Fig. 2.

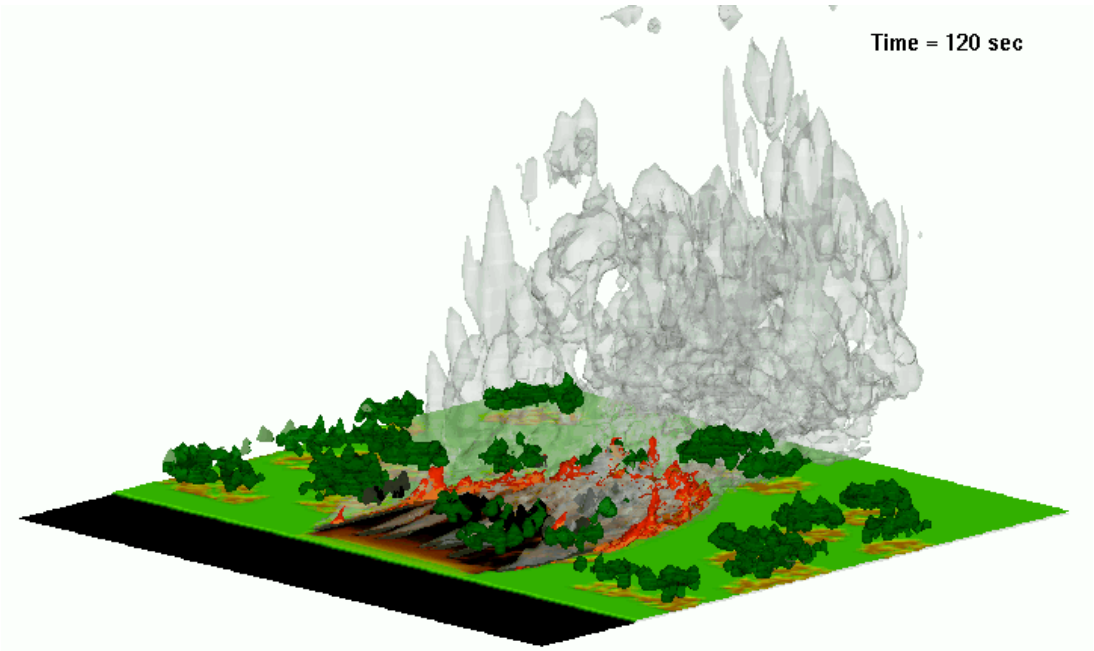

Figure 4. Image from the Patches simulation 120 seconds after ignition. The colors in this image are similar to those in Fig. 2.

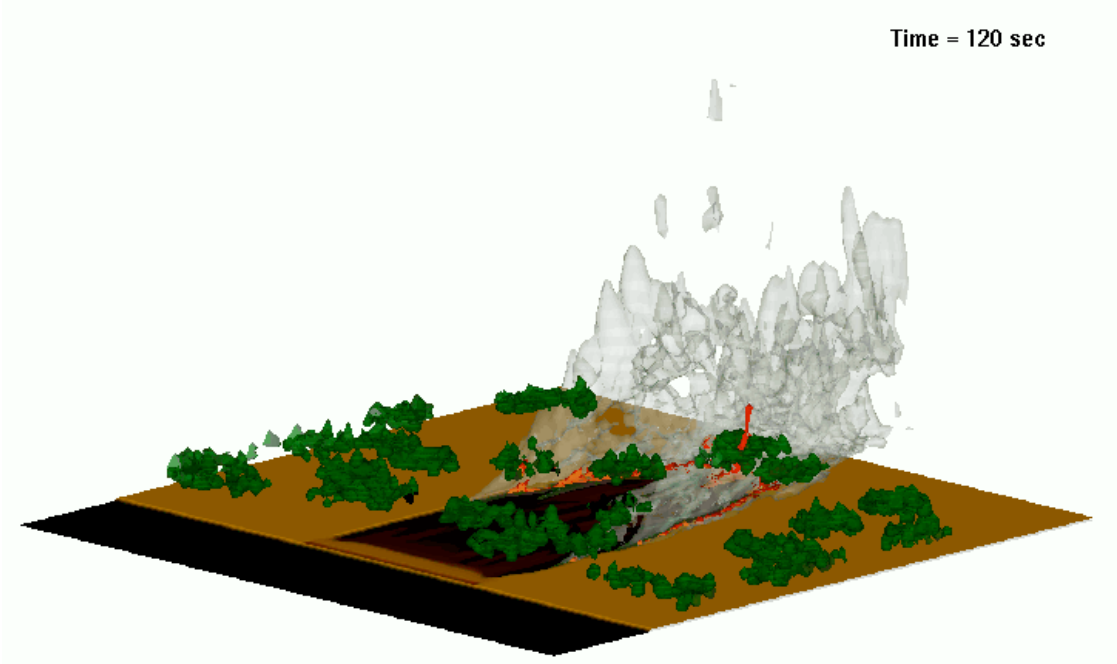

Figure 5. Image from the Patches, less ground fuel or PLGF simulation 120 seconds after ignition. The colors on the horizontal plane indicate bulk ground fuel density, with black being no fuel and brown being short grass and litter with a load that varies around .5 kg/m3 . The dark green isosurfaces show the tree locations, and the black isosurfaces show parts of the canopy that have been significantly burned. The orange, red, and grey isosurfaces indicate regions of hot gases.

simulation, but the grass in the understory has been cut in half (reducing the height and mass of the fuel). An image from this simulation is shown in Fig. 5. We refer to this simulation as the "Patch, less ground fuel" or "PLGF".

4. RESULTS

One way to compare the four simulations is to look at the rate of propagation of the fires. Fig. 6 shows the downwind propagation distances of the fire from the ignition point. From the data shown in this figure, it is possible to calculate the average rate of spread (slope of the lines shown) of the fires in each simulation. The spread rates range from 1.17 m/s for the Full forest simulation to 1.52 m/s for the PLGF simulation. The Thin and Patches simulations produced mean spread rates of approximately 1.47 m/s and 1.44 m/s, respectively. The spread rates of the fires in the simulations with similar ground fuels are grouped closely, while the spread of the fire in the lighter grasses is faster. This might indicate that the ground fuels are carrying the fire and controlling its ability to spread in these simulations, since the large variation in canopy structure does not seem to strongly affect the spread rate under these wind conditions. We intend to investigate the reason for this apparent lack of sensitivity to canopy structure in future research.

Fig. 7 through 12 are included to incite curiosity relative to the potential questions that could be addressed with tools like HIGRAD/FIRETEC. These figures are meant to show trends and illustrate interesting differences between the fire/atmosphere/fuel interaction with different canopy structures and at different locations within the canopy. They are not meant to be used to show details.

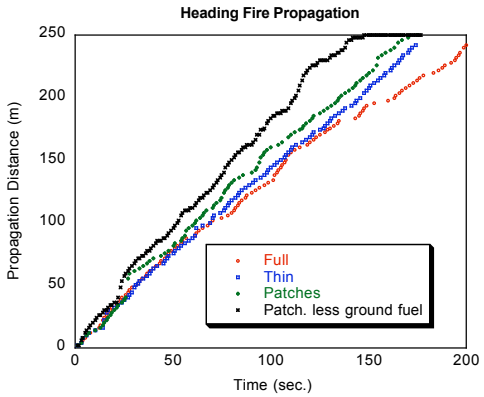

Figure 6. This figure shows the downwind propagation of the fire front for the four simulations.

For the purposes of generating the graphs in Fig. 7 through 12, we located three points (referred to as points 1, 2, and 3) in the canopy and tracked various quantities at these locations. In order to make it easier to compare these points, we chose them to be 12 m from the ground in three trees that have identical characteristics and were not removed from any of the simulations. The locations of these trees are shown in Fig. 7. The exact same locations were used in the other three simulations, even though the trees around them are different in the Full forest and Thin simulations. The trees that contain the

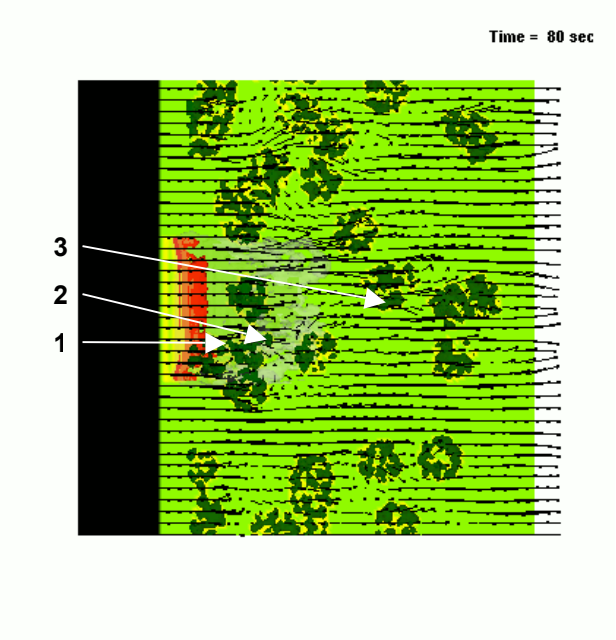

Figure 7. This image, from the Patches simulation, uses vectors to show the flow field 12 m from the ground. The ambient winds at the upper and lower left corners of the image are 6 m/s. The white arrows indicate the three locations (points) that are referred to in the text. The black region is an area where there is no fuel and the light green areas are the locations of the tall grass. The dark regions are isosurfaces of trees.

points of interest have the same trunk diameter (at breast height) of 29.4 cm, with a crown radius of 2.75 m. The height of the trees is 14.1 m, and the height to live crown is 8.5 m. The three points of interest are located one in each tree approximately 12 m from the ground. Some of the characteristics of the fuel, wind, and energy transfer at that location are plotted for each point in each simulation in Fig. 8 through 12.

The three graphs in Fig. 8 show the mass loss of the vegetation as a function of time. Each of the three graphs is associated with one of the three points, and contains 8 different sets of data points with interpolated curves drawn through them. These curves show the reduction of wood and water mass from the vegetation as the wood heats and cools. The burning model and moisture evaporation models that are used in FIRETEC are crude mixing limited models. We do not want to focus on the details of the mass loss rates, but instead provide a means of seeing the trends of the burning under the different circumstances. In each plot, we can see that the water begins to leave the vegetation at a faster rate than the wood. In the Full simulation at point 2 and Full, Thin and Patches simulations at point 3 the water is driven out completely. At point 1, some of the water is driven off, but the majority of the wood mass stays in tack. However, approximately 60 percent of the wood mass is lost from the Full forest at point 2 and 3, and about 65 percent in the Thin forest. There is less than 20 percent of the wood lost from any of the points in the Patches and PLGF simulations.

The three plots in Fig. 9 show the solid (for this purpose, “solid” includes wood and liquid water) temperature as functions of time. At point 1, none of the mean solid temperatures get above 375 K. The vegetation at point 2 in the Full forest is able to begin actively burning. The temperature reaches nearly 1200 K and remains above 1000 K for about 20 seconds. The temperatures at point 2 in the other simulations never get above 400 K. The temperatures at point 2 in the two Patchy simulations rise and fall off slowly, while the temperature at point 2 in the Thin simulation oscillates at a higher frequency. This oscillation is believed to be associated with wind oscillations. The temperatures at point 3 in the Thin and Full forest simulations indicate active burning since they reach temperatures of nearly 1100 K and 1000 K, respectively. Point 3 in the Patches simulation has a rise in temperature to approximately 475 K, then a decline in temperature and finally a second small rise and fall (peaking at approximately 350 K). The temperature at point 3 in the PLGF simulation grows slowly to about 400 K and declines slowly. These observations are consistent with the trends seen in Fig. 8.

The graphs in Fig. 10 show the bulk convective heating rates as a function of time. The convective heating at point 1 is minimal in all of the simulations. Since convective heating requires a difference in air and solid temperature, the lack of convective heating and low solid temperatures at point 1 indicate that this point is not in the path of the hot plume. This is partially due to the fact that it is relatively close to the ignition point of the fire. The ground fire may not have established itself sufficiently to force a strong, hot plume. There are two small oscillations in the convective heating in the Patches simulation, and a couple of very short durations where there is some heating in the Full and Thin cases. These heating episodes are attributed to different scale oscillations and fluctuation in the wind field as it interacts with the fire and canopy. The convective heating at point 2 shows stronger heating for all of the simulations, especially the Full forest simulation. In the Full simulation, there is a strong heating period associated with the hot plume being driven over the cooler vegetation, and then a strong cooling period associated with cooler ambient winds being driven over the burning tree after it is ignited. There are smaller amplitude heating and cooling periods for point 2 in the other simulations. The convective heating at point 3 in the PLGF simulation precedes the heating in the other simulations because the ground fire reaches this location faster, as seen in Fig. 6. The convective heating of the vegetation at point 3 in the other simulations is moderate in comparison to the Full case at point 2. This is probably due to the fact that the temperature of the solid rises at nearly the same rate as the air around it. As the plumes from the ground fires in these simulations pass by point 3, and the cooler ambient air blows on the vegetation, there is

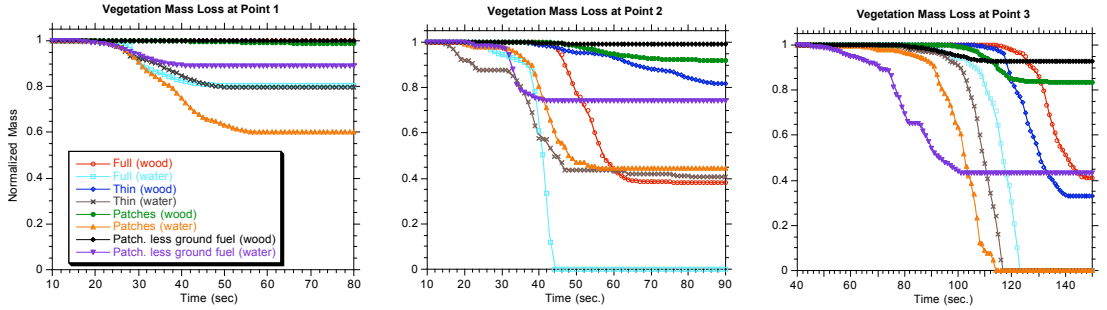

Figure 8. Plots of vegetation mass loss at points 1, 2, and 3 as a function of time since ignition.

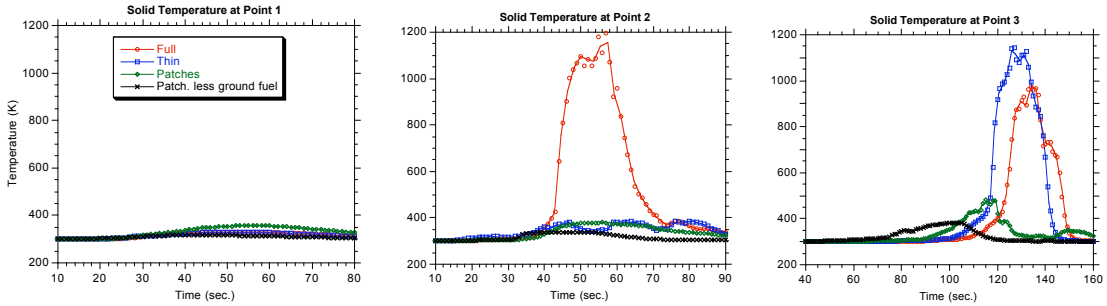

Figure 9. Plots of the solid temperature at points 1, 2, and 3 as a function of time since ignition.

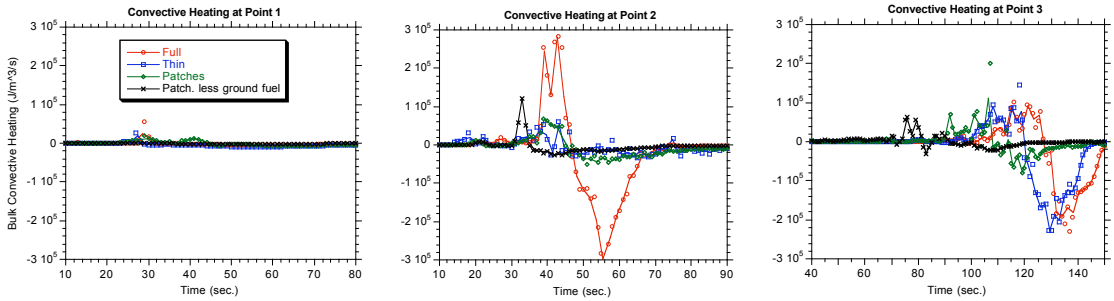

Figure 10. Plots of the bulk convective heating rate of the solid at points 1, 2, and 3 as a function of time since ignition.

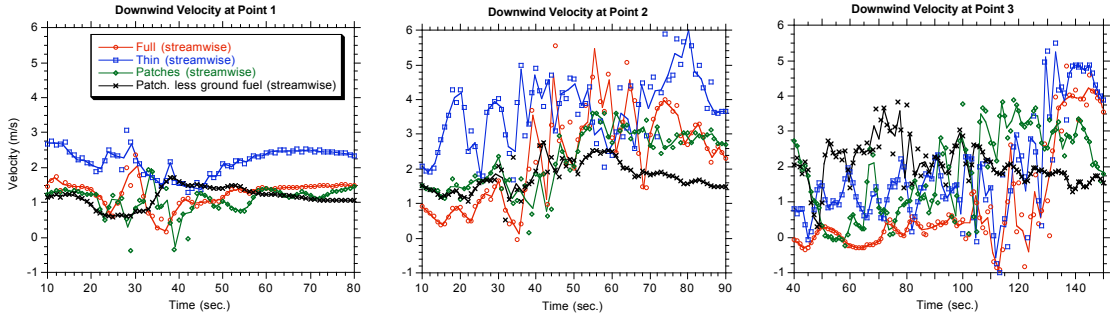

Figure 11. Plots of the downwind veloctity (in the x direction) at points 1, 2, and 3 as a function of time since ignition.

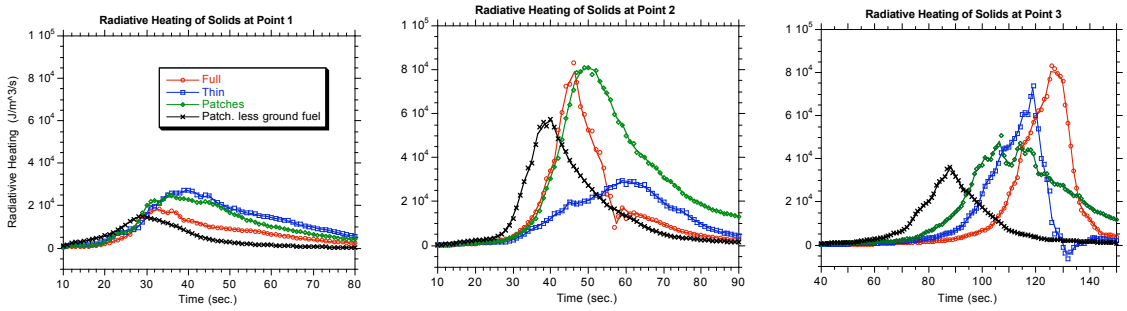

Figure 12. Plots of the bulk radiative heating rate of the solid at points 1, 2, and 3 as a function of time since ignition.

a strong convective cooling effect. This contributes to the incomplete burning in the Full and Thin simulations (seen in Fig. 8) and the intermediate cooling in the Patches simulation (seen in Fig. 9).

The three plots in Fig. 11 show the air velocity in the x direction (the downwind direction of the ambient wind) as functions of time. The trend is for the velocity to decrease as the ground fire approaches point 1, become turbulent when the fire is near (associated with the near field recirculations), and then regain strength as the fire passes by point 1. At point 2, the velocities are much more turbulent than at point 1. This may be caused by the fact that this point is farther into the forest, and so the flow is more perturbed by obstacles. The velocities in the Thin simulation are larger on average than in the other simulations at point 2. This is because the fewer and more dispersed trees in this simulation provide less drag in the canopy (especially since point 2 is near the leading edge of the forest), and thus less mean departure from the ambient 6 m/s wind. These large fluctuations are believed to be the driver in the oscillations in the solid temperature at point 2 in the Thin simulation as mentioned above (see Fig. 9). There is a clear increase in the velocities and their fluctuations in the other three simulations as the plume from the ground fire moves over Point 2, followed by a slow decline in the velocities as the plume moves past. This is because the plume is not only flowing up, but also in the direction of the ambient wind. The velocities at point 3 fluctuate strongly in all cases except the PLGF simulation. The turbulence is again associated with the interaction between the fire, atmosphere, and fuels. The mean values of the velocities grow as the plume nears point 3. The velocity in the PLGF case has a little higher mean value at point 3, and is less turbulent. This higher mean velocity may be caused by the fact that the upwind vertical plume is not as strong and does not block as much wind as in the other simulations. The difference in the strength of the velocity fluctuations between the Patches and PLGF simulations at point 3 is attributed to the fact that there is less heat being produced in the simulation with less ground fuel, and so less buoyancy driven turbulence.

The final figure, Fig. 12, shows the net bulk radiative heating rate of the solid as a function of time. In this text, we are defining the net bulk radiative heating rate as the energy absorbed by the solid from thermal radiation minus the thermal radiation that is emitted by the solid. The radiation heat transfer model in FIRETEC is very crude, and so we are intending the reader to look at the trends rather than the details of these graphs. The trend in the radiative heating rates at point 1 for all simulations is for the heating to increase as the fire heats up after ignition and as the ground fire approaches, and then fall off as the fire moves away. The lower values in the PLGF simulation are attributed to the lower intensity of the fire that moves under point 1 sooner (possibly before the fire has reached full intensity), and then moves away quicker than in the other cases. The lower heating rates in the Full forest may be caused by the increased radiative shielding caused by the additional trees (smaller mean optical path length). At point 2, the peak radiative heating rates are more than double what they were at point 1 for all but the Thin simulation. These

increased rates can be attributed to the fact that the ground fire is more intense by the time it reaches point 2. In addition, there are other burning trees that are radiating energy towards point 2. The Thin simulation does not show the same increase in radiative heating rate perhaps because the trees are much more dispersed, and so do not have as much radiative heating contribution to each other. The heating rate increasing faster than it falls off is thought to be due to the fact that the ground fires are still increasing in temperature as they approach point 2. The net bulk radiative heating rate in the Full case at point 3 is similar in magnitude to that at point 2. The heating rate in the Thin simulation at point 3 is much higher than at point 2. This difference is possibly due to the fact that more trees were ignited around point 3 than around point 2, and so the effect of having the trees dispersed is lessoned. The reduction in the radiative heating rate for the two patchy simulations at point 3 could be due to the fact that there are no trees just upwind of the patch of trees where point 3 is located, and so the majority of the trees in the patch itself do not burn significantly. This reduces the tree-to-tree radiation effects. An additional interesting feature shown in Fig. 12 are the negative values in the Thin simulation radiative heating rates at point 3. These values are associated with the fact that the solid temperature at point 3 is high, even after the ground fire has passed. As a result, the tree is actually radiating more energy than it is receiving for a short period of time (potentially igniting other trees).

5. CONCLUSIONS

In this text, we have introduced the use of HIGRAD/FIRETEC for simulating fires as they move through forests made of individual treelike fuel elements. HIGRAD/FIRETEC is not a high fidelity combustion model, and does not attempt to capture the details of the combustion process or the fine-scale details of the vegetation or the flow field. HIGRAD/FIRETEC does, however, model the physics of the important processes that drive a wildfire, and captures many of the complex interactions between fire, atmosphere and fuel.

To illustrate the use of this model for simulating forest canopies, we chose three different trees that each existed identically in four different simulations. By examining a set of critical characteristics of the atmosphere and solid fuel at a location 12 m above the ground in each of these trees in the various simulations, we can see indications of different phenomenon occurring as an effect of a tree's location with respect to the ignition point, other trees, and the understory vegetation.

The number of simulations presented here is not sufficient to provide conclusive results about all of the interdependencies that occur in the simulations, but they are sufficient to inspire many new questions and to guide future research directions.

In order for the information from this type of model to be of real value, we must find ways to compare the results with experiments and real fires. By making these comparisons, we can gain confidence in the aspects of the model that are working correctly and obtain critical information about the deficiencies of the model that need improvement. By recognizing differences between the model and real fire behavior, researchers will learn more about the interaction between the driving processes in wildfires.

6. REFERENCES

Linn, R. R., Transport model for Prediction of Wildfire Behavior, 1997, Los Alamos National Laboratory Scientific Report: LA13334-T.

Linn, R.R., J. Reisner, J. Colman, J. Winterkamp, "Studying Wildfire Using FIRETEC," *International Journal of Wildland Fires,* 11 pp. 1-14, (2002).

Reisner , J.M., S. Swynne, L. Margolin, and R.R. Linn, 1999, Coupled-Atmosphere Fire Modeling Using the Method of Averaging. (submitted to Monthly Weather Review, August 1999).

Reisner, J. M., D. A. Knoll, V. A. Mousseau, R.R. Linn, 2000, New Numerical Approaches for Coupled Atmosphere-Fire Models, Third Symposium on Fire and Forest Meteorology. January 2000, Long Beach, Ca